



HHS Public Access

Author manuscript

Pediatr Res. Author manuscript; available in PMC 2019 April 26.

Published in final edited form as:

Pediatr Res. 2019 March ; 85(4): 511–517. doi:10.1038/s41390-018-0215-5.

The aquaporin-4 inhibitor AER-271 blocks acute cerebral edema and improves early outcome in a pediatric model of asphyxial cardiac arrest

Jessica S. Wallisch^{1,4,5}, Keri Janesko-Feldman⁵, Henry Alexander⁵, Ruchira M. Jha^{1,5}, George W. Farr⁶, Paul R. McGuirk⁶, Anthony E. Kline^{2,5}, Travis C. Jackson^{1,5}, Marc F. Pelletier⁶, Robert S.B. Clark^{1,3,4,5}, Patrick M. Kochanek^{1,3,4,5}, and Mioara D. Manole^{*,3,4,5}

¹Department of Critical Care Medicine, University of Pittsburgh, Pittsburgh, PA

²Department of Physical Medicine and Rehabilitation, University of Pittsburgh, Pittsburgh, PA

³Department of Pediatrics, University of Pittsburgh, Pittsburgh, PA

⁴Children's Hospital of Pittsburgh of UPMC, Pittsburgh, PA

⁵Safar Center for Resuscitation Research, Pittsburgh, PA

⁶Aeromics, Inc., Cleveland, OH

Abstract

Background: Cerebral edema after cardiac arrest (CA) is associated with increased mortality and unfavorable outcome in children and adults. Aquaporin-4 mediates cerebral water movement and its absence in models of ischemia improves outcome. We investigated early and selective pharmacologic inhibition of aquaporin-4 in a clinically relevant asphyxial CA model in immature rats in a threshold CA insult that produces primarily cytotoxic edema in the absence of blood brain barrier permeability.

Methods: Postnatal day 16–18 Sprague-Dawley rats were studied in our established 9-min asphyxial CA model. Rats were randomized to aquaporin-4 inhibitor (AER-271) vs vehicle treatment, initiated at return of spontaneous circulation. Cerebral edema (% brain water) was the primary outcome with secondary assessments of the neurologic deficit score (NDS), hippocampal neuronal death, and neuroinflammation.

Results: Treatment with AER-271 ameliorated early cerebral edema measured at 3 h after CA vs. vehicle treated rats. This treatment also attenuated early NDS. In contrast to rats treated with

Users may view, print, copy, and download text and data-mine the content in such documents, for the purposes of academic research, subject always to the full Conditions of use:http://www.nature.com/authors/editorial_policies/license.html#terms

***Corresponding Author:** Mioara D. Manole, MD, Children's Hospital of Pittsburgh, 4401 Penn Avenue, Pittsburgh, PA 15224, Tele: (412) 692-7692, Fax: (412) 692-7464, mioara.manole@chp.edu.

Author Contributions: JSW, PMK and MDM were involved in study conception and design as well as statistical analysis. JSW, KJF and HA contributed to acquisition of animal data. GWF, PRM and MFP contributed to acquisition of drug level analysis. JSW, RMJ, AEK, TCJ, RSBC, PMK and MDM were involved with interpretation of data. JSW drafted the article and all authors revised it critically for important intellectual content and approved the final version for publication.

Disclosure: Drs. Farr, McGuirk, and Pelletier are employees of Aeromics, Inc., which provided AER-271 and performed drug level analysis but had no influence on study design, outcome assessment, statistical analysis, writing of the manuscript, or decision to submit for publication.

vehicle after CA, rats treated with AER-271 did not develop significant neuronal death or neuroinflammation as compared to sham.

Conclusion: Early post-resuscitation aquaporin-4 inhibition blocks the development of early cerebral edema, reduces early neurologic deficit, and blunts neuronal death and neuroinflammation post-CA.

Introduction

Cerebral edema after cardiac arrest (CA) is associated with increased mortality and unfavorable neurological outcomes (1–3). Asphyxial CA, the most common type of CA in children, is preceded by a period of hypoxemia which worsens the hypoxic-ischemic brain injury (4, 5). This global cerebral hypoxic-ischemic insult results in cellular energy failure which drives the formation of cytotoxic edema, traditionally thought of as a net intake of water due to osmotic gradients in the setting of an intact blood-brain barrier (BBB) (6).

The aquaporins (AQP) are a family of transmembrane water channel proteins that regulate the flow of water in various tissues and organs. AQP1, 4, and 9 are expressed within the central nervous system (CNS) with AQP4 having the largest contribution to brain water regulation (7). AQP4 is expressed on the astrocyte end-foot process and is concentrated at the perivascular and periependymal spaces, allowing bi-directional osmotically-mediated flow of water (8). It is thought to have an integral role in the development of cytotoxic cerebral edema (9, 10) as well as the clearance of vasogenic edema (11).

AQP4 is upregulated following CA (12) and temporally correlates with early post-resuscitation cerebral edema, although the changes in expression following isolated cerebral ischemia are equivocal (12, 13). Yet, in models of both focal and global cerebral ischemia, AQP4 knockout mice show reduced injury as measured by cerebral edema, intracranial pressure, infarct volume, area of restricted diffusion, and neuronal loss versus control mice (14–16).

These knockout models provide proof of concept regarding a potential new treatment strategy to mitigate the development of cerebral edema after CA, yet pharmacotherapy is necessary to translate these findings to patient care. A novel therapeutic agent was recently synthesized, which selectively inhibits AQP4. This investigational small molecule inhibitor, AER-271, reduces cytotoxic cerebral edema in models of water intoxication and stroke (Aeromics, Inc., personal communication). This pharmacological agent offers a clinically relevant method of AQP4 inhibition to investigate the role of AQP4 in pediatric asphyxial CA-related cerebral edema.

We propose that AQP4 serves as a key immediate vector for cerebral edema after CA in the developing brain. We hypothesize that AQP4 inhibition early after resuscitation using AER-271 will prevent the formation of cerebral edema and improve outcomes after experimental pediatric asphyxial CA. We propose to assess this therapy in the setting of a CA insult that specifically highlights cytotoxic edema and delayed neuronal death in order to delineate the pharmacokinetics of AER-271 and its effect on cerebral edema and neuronal death.

Methods

Animal Model

Studies were approved by the Institutional Animal Care and Use Committee at the University of Pittsburgh. Mixed-litter male post-natal day (PND) 16–18 Sprague-Dawley rats (Harlan Laboratory) weighing 30–45 grams were used in an established model of asphyxial CA in immature rats (17) to evaluate cerebral edema and outcome (Figure 1). We chose to assess the effect of AER-271 in a sex-homogenous cohort of male rats to eliminate the possible confounding effect of sex, as there are well described innate sex differences in cytotoxicity and programmed cell death. We studied the effect of AQP inhibition in a threshold insult of 9 min where no gross alterations of BBB permeability were observed, highlighting specifically cytotoxic edema in this model and not vasogenic edema.

Rats were anesthetized with 3% isoflurane/50% N₂O/balance O₂ then intubated with an 18-gauge angiocatheter and mechanically ventilated with anesthesia maintained using 1% isoflurane/50% N₂O/balance O₂. Femoral venous and arterial catheters were placed under sterile technique via inguinal cutdown. A subcutaneous (SQ) osmotic infusion pump (Alzet 2001D, Cupertino, CA) was implanted into the interscapular space in cohorts of rats with outcomes beyond 24 h (see section AER-271 and Pharmacokinetic Studies). Continuous monitoring was conducted with electrocardiography (EKG), arterial blood pressure, end-tidal CO₂ (ETCO₂), pulse oximetry, rectal temperature, and electroencephalography (EEG). Mechanical ventilation was titrated by ETCO₂ and arterial blood gas measurements.

At 2 min prior to asphyxia, vecuronium (1mg/kg, IV) was administered to stop respirations and N₂O was discontinued. The fraction of inspired oxygen (FiO₂) was reduced to 0.21 for one min and then asphyxia was induced by disconnecting the ventilator for 9 min resulting in CA. Resuscitation included reconnecting the ventilator with an FiO₂ of 1.0, administering epinephrine (0.005mg/kg, IV) and sodium bicarbonate (10mEq/kg, IV) to target normalization of arterial pH, and chest compressions until return of spontaneous circulation (ROSC). Shams underwent anesthesia, intubation, mechanical ventilation, vascular catheter placement, and had SQ drug infusion pumps implanted. At one h after resuscitation, vascular catheters were removed, rats were weaned from the ventilator and extubated, recovered from anesthesia, and returned to cages with lactating mothers and littermates prior to sacrifice.

AER-270/271 Bioanalytical Methods

AER-270 (Aeromics, Inc., Cleveland, OH) is a selective, partial antagonist of AQP4 identified using high-throughput screening. Inhibition of AQP4-mediated water movement was confirmed using cell cultures over-expressing AQP4 and subjected to osmotic stress. AER-271 is a phosphonate prodrug derivative of the parent compound AER-270. AER-271 is converted in vivo to AER-270 by endogenous phosphatases, and has markedly increased water solubility compared with the parent drug AER-270 (Aeromics Inc., personal communication). AER-271 is effective at reducing cerebral edema and improving outcomes in models of water intoxication and ischemic stroke (Aeromics, Inc., personal communication), and was recently reported to be effective in a model of cold ischemic storage in the setting of cardiac transplantation (18).

Rats were randomized to treatment with AER-271 versus vehicle (Tris base in saline). Table 1 summarizes the study groups, medication doses, and outcomes. An initial cohort (n=4/group) compared the efficacy of the intraperitoneal (IP) and intravenous (IV) routes where treatment was initiated at the time of ROSC with a loading bolus dose of 5mg/kg followed by a second bolus dose of 5mg/kg at 60 min post-ROSC. Serum drug levels were measured at 15, 80, and 180 min. A second cohort tested longer maintenance of drug therapy with a loading bolus dose of 5mg/kg at ROSC paired with a primed subcutaneous (SQ) osmotic continuous infusion pump (0.08mg/h x 24 h). Serum drug levels were measured at 1, 6, and 24 h (n=6).

Plasma levels of the active drug, AER-270 were analyzed using an integrated Shimadzu 8050 LC-MS/MS system (Shimadzu Scientific Instruments, Columbia, MD) at the Proteomics and Metabolomics Core, Lerner Research Institute, Cleveland Clinic Foundation, Cleveland, OH. Plasma proteins were first removed by 75% acetonitrile extraction and AER-37, a derivative of AER-270, introduced as an internal standard. Samples were analyzed by tandem LC-MS/MS using C18 reversed-phase chromatography with acetonitrile and ammonium carbonate as a counter-ion (Prodigy 2 × 150 mm, 5 μm 110A, Phenomenex, Torrance, CA). Mass analysis with Multiple Reaction Monitoring (MRM) utilized a triple-quadrupole mass spectrometer and ESI probe. The method gives reliable quantitation of AER-270 in the range of 0.5–1000 ng/mL. Target plasma levels of AER-270 were 70ng/mL based on therapeutic levels in a mouse ischemic stroke model (Aeromics, Inc., personal communication).

Cerebral Edema

To assess the effect of AER-271 on cerebral edema, rats (n=6/group at each time point) underwent CA and were randomized to treatment with AER-271 or vehicle (identical volume and administration time) at resuscitation. The rats were sacrificed at 3, 6, and 24 h post-CA for measurement of cerebral edema using the wet-dry weight method. Naïve rats provided normative data for control. Following decapitation, whole brains were extracted from the cranium and the olfactory bulbs and cerebellum were removed. Brains were weighed (wet weight) then dried in glass vials at 110 degrees Celsius (°C) for 72 h. At 72 h, the dry weight measurement was performed and cerebral percent brain water (%BW) was calculated as (wet weight – dry weight)/wet weight × 100. Edema was calculated as [(injury %BW – naïve %BW)/naïve %BW] × 100.

Acute Neurologic Deficit

To assess the effect of AER-271 on acute neurological deficit and neuropathology, a separate cohort of rats (n=6/group) underwent CA or sham surgery with vehicle control. The two CA groups were randomized to treatment with AER-271 or vehicle. An established neurologic deficit score (NDS) was used to assess rats' functional status at 3, 24, 48, and 72 h post-CA (19). A blinded technician assessed functional status in categories of general behavior, cranial nerve reflexes, motor, sensory, and coordination for a total score ranging from 0–500 points with higher score indicative of more severe injury. General behavior (max 200 points) evaluated consciousness and respirations. The cranial nerve reflexes (max 100 points) included testing of the olfactory, vision, corneal, whisker movement, and hearing. Motor and

sensory deficits (max 50 points each) were documented in each forepaw, hindpaw, and tail. Lastly, coordination deficit (max 100 points) was assessed as ability to walk along a ledge, reaching with forepaws when lifted by tail, stopping at the edge of a table, and righting reflex.

Histology

At 72 h post-CA, rats (n=6/group) were anesthetized with 3% isoflurane/50% N₂O/balance O₂ and transcardially perfused with 50mL of ice-cold heparinized saline followed by 50mL of 10% buffered formalin. Following decapitation, the brains were excised and stored in formalin for a minimum of 24 h. Paraffin embedded brains were cut into 5 µm coronal sections using a microtome.

Neuronal injury was assessed using hematoxylin and eosin (H&E) stained sections. Hippocampal images were obtained at 10× magnification (NIS-Elements software, Nikon Eclipse 90i microscope, Melville, NY). A blinded observer quantified the eosinophilic pyknotic neurons within the hippocampal CA1 region. The length of the CA1 region was measured for each sample, and the pyknotic neuronal counts were indexed per 0.1mm length of CA1 hippocampus.

Fluorochrome B (Millipore Sigma, Burlington, MA) stained sections served as a second assessment of neuronal degeneration (17). Sections were deparaffinized in xylene then serially immersed in 100% alcohol, 1% sodium hydroxide in an 80% alcohol solution, 70% alcohol, and 0.06% potassium permanganate. Slides were washed in distilled water then immersed in 0.0006% working Fluorochrome B solution (Fluorochrome B, 0.1% acetic acid, DAPI) on a shaker protected from light for 30 min. After a series of distilled water washes, the slides were dried on a slide warmer at 50°C for 10 min, dipped in xylene, and then coverslipped with DPX mounting medium. Images were captured at 10× magnification and a blinded observer quantified the fluorochrome positive neurons within the hippocampal CA1 region. The length of the CA1 region was measured for each sample, and the Fluorochrome neuronal counts were indexed per 0.1mm length of CA1 hippocampus.

Neuroinflammation was evaluated by assessing the microglial response using Iba1 staining. Slides were deparaffinized in xylene then dehydrated in 100% ethanol followed by 95% ethanol. Antigen retrieval was completed (10X antigen decloaker, Biocare Medical, Pacheco, CA) and the endogenous peroxidases were blocked with hydrogen peroxide for 30 min before blocking in 3% normal goat serum for 30 minutes. Sections were incubated at 4°C overnight with rabbit polyclonal anti-Iba1 antibody (1:250, Wako Chemicals, Richmond, VA). The following day, slides were incubated in biotinylated goat anti-rabbit secondary antibody for 1 h at room temperature (Vectastain ABC Kit, Vector Labs, Burlingame, CA). Sections were subsequently incubated in avidin-biotin complex for 1 h at room temperature (Vectastain ABC Kit). 3,3'-diaminobenzidine (DAB) was applied (10 min) followed by hematoxylin counterstain. After serial immersion in 70% ethanol, 95% ethanol, 100% ethanol, and xylene, slides were coverslipped with Permount mounting medium. Images were captured at 20× magnification from a standardized region of interest (ROI) centering on the CA1 hippocampus immediately superior to the dentate gyrus and a blinded observer quantified the Iba1 positive microglia which were indexed for the area of ROI (per mm²).

Statistical Analysis

Student t-test or one-way ANOVA with Student Newman Keuls (SNK) post-hoc test (presented as mean \pm standard error of the mean) and Mann-Whitney or ANOVA on ranks (presented as median [interquartile range]) were used to analyze and/or display normally and non-normally distributed data, respectively. Data with multiple measurements were analyzed by two-way repeated measures ANOVA with SNK. One statistical outlier was determined using Thompson Tau test and removed from 3 h edema analysis. Alpha = 0.05 was considered statistically significant.

Results

Physiologic Data

Combined baseline parameters including heart rate, mean arterial pressure (MAP), and temperature were similar between treatment groups. For injury groups, the heart rate ($p=0.21$), mean arterial pressure ($p=0.64$), temperature ($p=0.85$), and CPR duration ($p=0.06$) were not different at any time point (Supplemental Table S1 (online)).

There were no differences in baseline or subsequent pH, ETCO_2 , PaCO_2 , PaO_2 , or HCO_3 between injury groups. Mean serum lactate, osmolarity, sodium, potassium, chloride, ionized calcium, glucose, and hematocrit did not vary by treatment group for injury animals across the model (all comparisons NS).

AER-271 Pharmacokinetics

After AER-271 bolus administration at 0 and 60 min post-ROSC, plasma levels of the parent drug AER-270 reached therapeutic levels rapidly using either IV or IP route. Levels peaked following IV administration and showed less variability via IP administration (Supplemental Figure S1a (online)). Thus we selected the IP route for the loading dose in all subsequent studies of efficacy. Therapeutic drug levels were confirmed in the cerebral edema cohort of rats ($726.16 \text{ ng/mL} \pm 114.22$ at 180 min after CA).

An IP loading bolus followed by continuous SQ infusion rapidly attained and maintained therapeutic drug levels through 24 h (Supplemental figure S1b (online)). Therapeutic drug levels were confirmed in the cerebral edema cohort of rats (1475.99 ± 305.11 and $1699.37 \pm 181.50 \text{ ng/mL}$ at 6 and 24 h, respectively).

Cerebral Edema

At 3 h post-CA %BW was increased in CA-vehicle-treated vs. naïve rats ($83.84 [83.16, 83.39]$ vs. $83.17 [82.68, 83.28]$ respectively, $p<0.05$) (Figure 2a). AER-271 treatment prevented the acute increase in %BW ($83.29 [83.16, 83.39]$, CA-AER-271 vs naïve NS) and reduced the amount of edema present at 3 h by 82.1%, returning %BW nearly to the naïve value. %BW in the injury cohorts decreased towards levels of naïve rats at 6 h and 24 h post-CA (Figure 2b-c).

Acute Neurologic Deficit

At 3 h post-CA, both injury groups showed a significant deficit vs. sham (325.00 ± 30.00 , 261.67 ± 20.56 , 0.83 ± 0.83 ; CA-vehicle, CA-AER-271, and sham, respectively, $p < 0.001$ CA-vehicle and CA-AER-271 vs sham) (Figure 3a). CA-AER-271 rats had a 20% lower NDS compared to CA-vehicle ($p < 0.001$). At 24–72 h post-CA, overall NDS improved with no significant injury effect remaining. An exploratory post-hoc analysis of the 3 h NDS component subgroups did not reveal a treatment effect on NDS subgroup (Figure 3b).

Histology

Hippocampal CA1 neurons are vulnerable to CA in our model (Figure 4), and treatment with AER-271 resulted in a 43% reduction in pyknotic degenerating neurons on H&E compared to vehicle, which was not different from sham (Figure 5). This reduction in neuronal damage with AER-271 was corroborated by a 49% reduction in CA1 hippocampal Fluorojade positivity.

The CA1 hippocampal microglial response was increased after CA in vehicle, but once again not in the CA-AER-271 treatment group which had a 55% reduction in Iba1 positivity as compared to vehicle, suggesting attenuation of neuroinflammation with treatment.

Discussion

Cerebral edema is a well-known consequence of global brain ischemia resulting from CA, particularly in the setting of asphyxial CA in infants and children (3, 20). However, cerebral edema has been a relatively overlooked potential therapeutic target for neuroprotection after CA. Pediatric studies in the 1980s-1990s suggested that although cerebral edema and resultant intracranial hypertension develop after asphyxial CA, conventional treatment approaches using intracranial pressure monitoring and hyperosmolar therapy did not impact neurological outcome (20, 21). Additionally, studies in adult patients found that delayed treatment of elevated ICP after CA is unlikely to improve outcome (22). These studies directed the field of CA away from targeting cerebral edema as a neuroprotective approach for decades.

However, some studies suggest that setting a threshold for treatment at severe cerebral edema that results in intracranial hypertension might be too late, and early treatment of edema might be beneficial. In fact, preclinical models of CA in primates observed vegetative neurological outcome despite the absence of elevated ICP in monkeys subjected to 16 min of complete global ischemia (23). More recently, a few studies have suggested that mitigating earlier post-resuscitation brain edema may represent a therapeutic opportunity. Nakayama et al showed that Conivaptan, a selective arginine vasopressin V1a and V2 receptor antagonist, and hypertonic saline attenuate global cerebral edema at 24 h after KCl-induced CA in mice via effects on AQP4 (24, 25). The 8 min KCl-induced CA produced BBB disruption, unlike our model of asphyxial CA. Moreover, functional outcome and neuronal death were not assessed in that study. Other pathways and mechanisms of edema management including therapeutic hypothermia and the sulfonyl urea receptor-1 (SUR-1) antagonist glyburide have also attenuated cerebral edema at 24 h after a 7 min KCl-induced CA in mice (26). However,

acute brain edema develops extremely rapidly after CA, as early as 3 h after resuscitation as shown in our studies, and hypothermia takes time to induce, as does post-ischemic SUR-1 protein transcription, which is not present at resting state (27, 28). AQP4 is constitutively expressed and allows for immediate water movement following injury, and thus inhibition of AQP4 by AER-271 may be suited to immediately block edema, also affording an opportunity to examine the impact of early treatment targeting edema on subsequent neuronal death and neuroinflammation.

Our work represents the first reported molecularly targeted pharmacologic inhibition of AQP4 after CA. Additionally, our work is the first reported investigation using a pediatric model and takes into account developmental differences that would allow for better translation and applicability to children with asphyxial CA. Notably, treatment with AER-271 was well tolerated with no apparent effect on haemodynamics or serum chemistry. AER-271 prevented the development of acute cerebral edema which is consistent with the aforementioned prior work in AQP4 knockout models of asphyxia/ischemia. In our model of asphyxial CA, we previously reported no disruption of the BBB after a 9 min insult as assessed using multiple approaches (6). This global hypoxic-ischemic injury, thus, highlights cytotoxic cerebral edema. Given that AQP4 is constitutively present, it would allow for immediate water movement following injury, supporting the biologic plausibility of using an AQP4 inhibitor to mitigate the development of brain edema early post-resuscitation.

We selected to test the AQP4 antagonist in a setting that produces primarily cytotoxic edema and delayed neuronal death in the absence of vasogenic edema, to provide a robust therapeutic opportunity for this specific mechanism. Our model mimics a number of important features of clinical brain ischemia: chest compression, use of epinephrine, and whole body insult. Our model produces a threshold insult with respect to neurologic injury. Despite the mild and transient nature of the cerebral edema and early post-resuscitation neurologic deficit that develops after a 9 min asphyxial CA, this injury produces neuronal death and longer lasting spatial memory acquisition deficits (17). In both the edema and acute NDS assessments, treatment with AER-271 resulted in improvement at the earliest time points (3 h post-CA). In this threshold model, both early edema and increased NDS are transient, limiting them as potential therapeutic targets at later time points (6–24 h for edema; 24–72 h for NDS). Inhibiting early cerebral edema formation also, surprisingly, attenuated CA1 hippocampal neuronal death at 72 h. It is unclear whether the effect of AER-271 on early edema is mediating the effect on neurodegeneration. Assessment of AER-271 in insults of greater severities where a higher degree of edema is produced are warranted. In this initial evaluation of the effect of AER-271 on behavioral and histological outcome, we assessed an acute time point of 72 h. We have not yet carried out studies testing more sophisticated behavioral assessments at longer time points, such as Morris water maze, fear conditioning, or open field, however, studies of those outcomes are planned for future experiments.

Neuroinflammation has been linked with neuronal death. In general, neuronal ischemic injury leads to microglial activation, and microglial activation and cytokine release have been associated with secondary neuronal death (30) with key developmental differences in these interactions (31). Our data revealed a reduction in the microglial response with AQP4

inhibition following CA that is supported by prior work with AQP4-null mice in a model of neuroinflammation which also showed reduced microglial activation (32). Given that microglia do not express AQP4 (32, 33), we propose that this is the result of a direct neuroprotective effect with a reduced secondary microglial response, which has also been seen in other studies (34–38). However, as AQP4 is expressed on T lymphocytes, as was recently shown in a model of cardiac transplantation (18), it is also possible that effects on neuroinflammation could be mediated by T lymphocyte interactions with microglia. Alternatively, we cannot exclude the possibility that AER-271 modulates cytokines or other inflammatory mediators of astrocyte activation that could alter the microglial response (39) by some means unrelated to its activity against AQP4.

Our study has limitations including the exploratory nature of some of our outcomes. We powered our study to detect differences in our primary outcome of brain edema in the absence of BBB disruption. A larger sample size would be needed to confirm histological evidence that AER-271 is neuroprotective relative to vehicle. Studies with a longer insult duration in a CA model with sustained edema would also be informative. We aimed to initially assess the effect of AQP4 blockade in an insult with primarily cytotoxic edema. The effect of AER-271 on vasogenic edema is not completely understood, and clearance of vasogenic edema may even be inhibited by AQP4 blockade, with loss of net overall efficacy. In light of these mechanisms, the effects of AER-271 in CA insults of longer durations, where a combination of cytotoxic and vasogenic edema exists, may or may not be greater. Assessment of AER-271 across a spectrum of insult severities is therefore warranted. Additionally, while promising, our findings need validation in a pediatric knockout model to determine whether the benefits derived from AER-271 treatment are related to off-target effects. Although AER-270 crosses the BBB and reaches therapeutic brain tissue levels, the mechanism by which the active drug inhibits AQP4 remains proprietary. However, the potential of a selective AQP4 antagonist for clinical trials supports these preliminary investigations. AQP4 is present in a number of other tissues and organs and it was outside the scope of our study to determine if any extra-CNS effects of AQP4 inhibition contributed to overall survival and functional outcome. For example, germane to CA, AQP4 is present in the myocardium and AQP4 knockout mice have been shown to have reduced infarct size in models of myocardial ischemia reperfusion (40). Additional investigation into the molecular basis for AQP4 inhibition, whether early AQP4 inhibition translates into improved long term outcomes, and to characterize the link between neuronal death and neuroinflammation are warranted. To avoid the confounding effect of sex on cytotoxicity we assessed the effect of AER-271 in male rats only. Future studies in female rats are also warranted. Finally, as previously mentioned, asphyxial CA may differ from ventricular fibrillation and arrests of cardiac origin with regard to brain pathophysiology, as suggested in recent studies showing enhanced brain injury in the setting of asphyxia (4). Given that these studies were carried out in asphyxial CA and in a pediatric model could potentially limit generalizability across all of CA.

In conclusion, AQP4 inhibition with AER-271 shows promise as a targeted therapy after asphyxial-CA in the developing rat brain for reduction in acute cerebral edema and improved neurological outcome. Therapeutic levels in the target range were rapidly achieved and maintained without apparent side effects. Attenuation of acute brain edema with an

AQP4 partial antagonist exhibits favorable consequences on neurological deficits, delayed neuronal death, and neuroinflammation. This suggests that targeting acute edema may represent a therapeutic opportunity after pediatric CA. Given the importance of asphyxial CA in the field of pediatrics and the emerging epidemic of asphyxial CA in adults as a result of the opioid epidemic, this agent warrants additional pre-clinical exploration.

Supplementary Material

Refer to Web version on PubMed Central for supplementary material.

Acknowledgements:

We are grateful to Aeromics, Inc. for providing us with AER-271. We thank Lee Ann New for providing technical assistance in NDS assessment.

Statement of Financial Support: The study was supported by grants from the Laerdal Foundation (JSW); NIH NICHD T32 HD040686 (JSW), R01HD069620 (AEK), and 5R01HD075760 (MDM); and NIH NINDS 1K23NS101036 (RMJ), R01NS084967 (AEK), R21NS098057 (TCJ), R01NS084604 (RSBC), and 1R01NS087978 (PMK).

References

- Hanning U, Bernhard Sporns P, Lebiez P, et al. 2016 Automated assessment of early hypoxic brain edema in non-enhanced CT predicts outcome in patients after cardiac arrest. *Resuscitation* 104:91–94. [PubMed: 27036663]
- Langkjaer S, Hassager C, Kjaergaard J, et al. 2015 Prognostic value of reduced discrimination and oedema on cerebral computed tomography in a daily clinical cohort of out-of-hospital cardiac arrest patients. *Resuscitation* 92:141–147. [PubMed: 25882783]
- Rafaat KT, Spear RM, Kuelbs C, Parsapour K, Peterson B 2008 Cranial computed tomographic findings in a large group of children with drowning: diagnostic, prognostic, and forensic implications. *Pediatr Crit Care Med* 9:567–572. [PubMed: 18838936]
- Uray T, Lamade A, Elmer J, et al., University of Pittsburgh Post-Cardiac Arrest S 2018 Phenotyping Cardiac Arrest: Bench and Bedside Characterization of Brain and Heart Injury Based on Etiology. *Crit Care Med* Epub ahead of print.
- Vaagenes P, Safar P, Moossy J, et al. 1997 Asphyxiation versus ventricular fibrillation cardiac arrest in dogs. Differences in cerebral resuscitation effects--a preliminary study. *Resuscitation* 35:41–52. [PubMed: 9259060]
- Tress EE, Clark RS, Foley LM, et al. 2014 Blood brain barrier is impermeable to solutes and permeable to water after experimental pediatric cardiac arrest. *Neurosci Lett* 578:17–21. [PubMed: 24937271]
- Connolly DL, Shanahan CM, Weissberg PL 1998 The aquaporins. A family of water channel proteins. *Int J Biochem Cell Biol* 30:169–172. [PubMed: 9608669]
- Nielsen S, Nagelhus EA, Amiry-Moghaddam M, Bourque C, Agre P, Ottersen OP 1997 Specialized membrane domains for water transport in glial cells: high-resolution immunogold cytochemistry of aquaporin-4 in rat brain. *J Neurosci* 17:171–180. [PubMed: 8987746]
- Verkman AS, Yang B, Song Y, Manley GT, Ma T 2000 Role of water channels in fluid transport studied by phenotype analysis of aquaporin knockout mice. *Exp Physiol* 85 Spec No:233S–241S. [PubMed: 10795927]
- Yang B, Zador Z, Verkman AS 2008 Glial cell aquaporin-4 overexpression in transgenic mice accelerates cytotoxic brain swelling. *J Biol Chem* 283:15280–15286. [PubMed: 18375385]
- Papadopoulos MC, Manley GT, Krishna S, Verkman AS 2004 Aquaporin-4 facilitates reabsorption of excess fluid in vasogenic brain edema. *FASEB J* 18:1291–1293. [PubMed: 15208268]
- Xiao F, Arnold TC, Zhang S, et al. 2004 Cerebral cortical aquaporin-4 expression in brain edema following cardiac arrest in rats. *Acad Emerg Med* 11:1001–1007. [PubMed: 15466140]

13. Akdemir G, Kaymaz F, Gursoy-Ozdemir Y, Akalan N, Akdemir ES 2016 The time course changes in expression of aquaporin 4 and aquaporin 1 following global cerebral ischemic edema in rat. *Surg Neurol Int* 7:4. [PubMed: 26862443]
14. Akdemir G, Ratelade J, Asavapanumas N, Verkman AS 2014 Neuroprotective effect of aquaporin-4 deficiency in a mouse model of severe global cerebral ischemia produced by transient 4-vessel occlusion. *Neurosci Lett* 574:70–75. [PubMed: 24717641]
15. Katada R, Akdemir G, Asavapanumas N, Ratelade J, Zhang H, Verkman AS 2014 Greatly improved survival and neuroprotection in aquaporin-4-knockout mice following global cerebral ischemia. *FASEB J* 28:705–714. [PubMed: 24186965]
16. Yao X, Derugin N, Manley GT, Verkman AS 2015 Reduced brain edema and infarct volume in aquaporin-4 deficient mice after transient focal cerebral ischemia. *Neurosci Lett* 584:368–372. [PubMed: 25449874]
17. Fink EL, Alexander H, Marco CD, et al. 2004 Experimental model of pediatric asphyxial cardiopulmonary arrest in rats. *Pediatr Crit Care Med* 5:139–144. [PubMed: 14987343]
18. Ayasoufi K, Kohei N, Nicosia M, et al. 2017 Aquaporin 4 blockade improves survival of murine heart allografts subjected to prolonged cold ischemia. *Am J Transplant Epub ahead of print.*
19. Shaik JS, Poloyac SM, Kochanek PM, et al. 2015 20-Hydroxyeicosatetraenoic Acid Inhibition by HET0016 Offers Neuroprotection, Decreases Edema, and Increases Cortical Cerebral Blood Flow in a Pediatric Asphyxial Cardiac Arrest Model in Rats. *J Cereb Blood Flow Metab* 35:1757–1763. [PubMed: 26058691]
20. Sarnaik AP, Preston G, Lieh-Lai M, Eisenbrey AB 1985 Intracranial pressure and cerebral perfusion pressure in near-drowning. *Crit Care Med* 13:224–227. [PubMed: 3979068]
21. Le Roux PD, Jardine DS, Kanev PM, Loeser JD 1991 Pediatric intracranial pressure monitoring in hypoxic and nonhypoxic brain injury. *Childs Nerv Syst* 7:34–39. [PubMed: 2054806]
22. Safar P 1986 Cerebral resuscitation after cardiac arrest: a review. *Circulation* 74:IV138–153. [PubMed: 3536160]
23. Bleyaert AL, Nemoto EM, Safar P, et al. 1978 Thiopental amelioration of brain damage after global ischemia in monkeys. *Anesthesiology* 49:390–398. [PubMed: 103466]
24. Nakayama S, Amiry-Moghaddam M, Ottersen OP, Bhardwaj A 2016 Conivaptan, a Selective Arginine Vasopressin V1a and V2 Receptor Antagonist Attenuates Global Cerebral Edema Following Experimental Cardiac Arrest via Perivascular Pool of Aquaporin-4. *Neurocrit Care* 24:273–282. [PubMed: 26732270]
25. Nakayama S, Migliati E, Amiry-Moghaddam M, Ottersen OP, Bhardwaj A 2016 Osmotherapy With Hypertonic Saline Attenuates Global Cerebral Edema Following Experimental Cardiac Arrest via Perivascular Pool of Aquaporin-4. *Crit Care Med* 44:e702–710.
26. Nakayama S, Taguchi N, Isaka Y, Nakamura T, Tanaka M 2017 Glibenclamide and Therapeutic Hypothermia Have Comparable Effect on Attenuating Global Cerebral Edema Following Experimental Cardiac Arrest. *Neurocrit Care Epub ahead of print.*
27. Jha RM, Puccio AM, Chou SH, et al. 2017 Sulfonylurea Receptor-1: A Novel Biomarker for Cerebral Edema in Severe Traumatic Brain Injury. *Crit Care Med* 45:e255–e264. [PubMed: 27845954]
28. Simard JM, Woo SK, Schwartzbauer GT, Gerzanich V 2012 Sulfonylurea receptor 1 in central nervous system injury: a focused review. *J Cereb Blood Flow Metab* 32:1699–1717. [PubMed: 22714048]
29. Stokum JA, Gerzanich V, Simard JM 2016 Molecular pathophysiology of cerebral edema. *J Cereb Blood Flow Metab* 36:513–538. [PubMed: 26661240]
30. Kaushal V, Schlichter LC 2008 Mechanisms of microglia-mediated neurotoxicity in a new model of the stroke penumbra. *J Neurosci* 28:2221–2230. [PubMed: 18305255]
31. Bhalala US, Koehler RC, Kannan S 2014 Neuroinflammation and neuroimmune dysregulation after acute hypoxic-ischemic injury of developing brain. *Front Pediatr* 2:144. [PubMed: 25642419]
32. Li L, Zhang H, Varrin-Doyer M, Zamvil SS, Verkman AS 2011 Proinflammatory role of aquaporin-4 in autoimmune neuroinflammation. *FASEB J* 25:1556–1566. [PubMed: 21257712]

33. Liang R, Yong S, Huang X, Kong H, Hu G, Fan Y 2016 Aquaporin-4 Mediates the Suppressive Effect of Lipopolysaccharide on Hippocampal Neurogenesis. *Neuroimmunomodulation* 23:309–317. [PubMed: 28427055]
34. Drabek T, Janata A, Jackson EK, et al. 2012 Microglial depletion using intrahippocampal injection of liposome-encapsulated clodronate in prolonged hypothermic cardiac arrest in rats. *Resuscitation* 83:517–526. [PubMed: 21970817]
35. Grace PM, Shimizu K, Strand KA, et al. 2015 (+)-Naltrexone is neuroprotective and promotes alternative activation in the mouse hippocampus after cardiac arrest/cardiopulmonary resuscitation. *Brain Behav Immun* 48:115–122. [PubMed: 25774010]
36. Shi X, Li M, Huang K, et al. 2017 HMGB1 binding heptamer peptide improves survival and ameliorates brain injury in rats after cardiac arrest and cardiopulmonary resuscitation. *Neuroscience* 360:128–138. [PubMed: 28778700]
37. Wang QY, Sun P, Zhang Q, Yao SL 2015 Minocycline attenuates microglial response and reduces neuronal death after cardiac arrest and cardiopulmonary resuscitation in mice. *J Huazhong Univ Sci Technolog Med Sci* 35:225–229. [PubMed: 25877356]
38. Wang W, Lu R, Feng DY, Liang LR, Liu B, Zhang H 2015 Inhibition of microglial activation contributes to propofol-induced protection against post-cardiac arrest brain injury in rats. *J Neurochem* 134:892–903. [PubMed: 26016627]
39. Ikeshima-Kataoka H 2016 Neuroimmunological Implications of AQP4 in Astrocytes. *Int J Mol Sci* 17.
40. Rutkovskiy A, Valen G, Vaage J 2013 Cardiac aquaporins. *Basic Res Cardiol* 108:393. [PubMed: 24158693]

Phase:	Preparation & Monitoring	Pre-Arrest	Asphyxia → Cardiac Arrest	Resuscitation	Post-Cardiac Arrest Care	
Procedures/ Medications:	<ul style="list-style-type: none"> Anesthesia induction Endotracheal intubation & mechanical ventilation Inguinal cutdown for femoral venous and arterial catheter placement Subcutaneous osmotic drug pump implantation as indicated 	<ul style="list-style-type: none"> Vecuronium ↓ FIO₂ to 0.21 	<ul style="list-style-type: none"> Ventilator disconnected 	<ul style="list-style-type: none"> Resume mechanical ventilation ↑ FIO₂ to 1.0 Epinephrine Sodium bicarbonate Rapid manual chest compression Treatment initiated at ROSC 	<ul style="list-style-type: none"> Vascular catheters removed Mechanical ventilation weaned Extubation Post-anesthesia care and recovery 	
Monitoring:	Temperature	Blood Pressure	Electrocardiography	Electroencephalography	Pulse Oximetry	End-tidal CO ₂
	ABG: Baseline					ABG: 10, 30, 60 minutes post-ROSC

Figure 1.
Pediatric asphyxial cardiac arrest model.

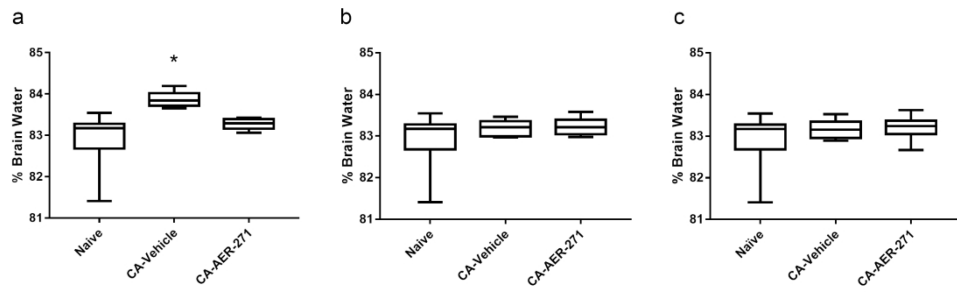


Figure 2.

Assessment of percent brain water (%BW) at 3 hours, 6 hours, and 24 hours after cardiac arrest. (a) Treatment with AER-271 prevented the acute increase in %BW at 3 h postcardiac arrest that was detected in vehicle vs naïve. (b & c) Edema was resolved in all injury groups by 6 and 24 h post-cardiac arrest. Assessed by one-way ANOVA on Ranks with Dunn's Method for pairwise multiple comparisons. Median [IQR]; * $p < 0.05$ CA-vehicle vs sham.

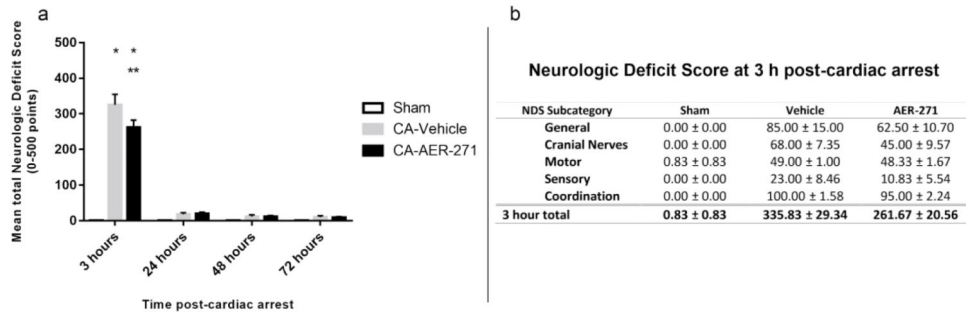


Figure 3. Assessment of early functional outcome by Neurologic Deficit Score (NDS). (a) Mean total NDS at 3 hours, 24 hours, 48 hours, and 72 hours post-cardiac arrest by treatment group. Assessed by two-way repeated measures ANOVA with Student Newman Keuls post-hoc test. Mean ± standard error of the mean; *p<0.001 vs sham, **p<0.001 vs vehicle. (b) Mean NDS subcategory scores at 3 hours post-cardiac arrest by treatment group.

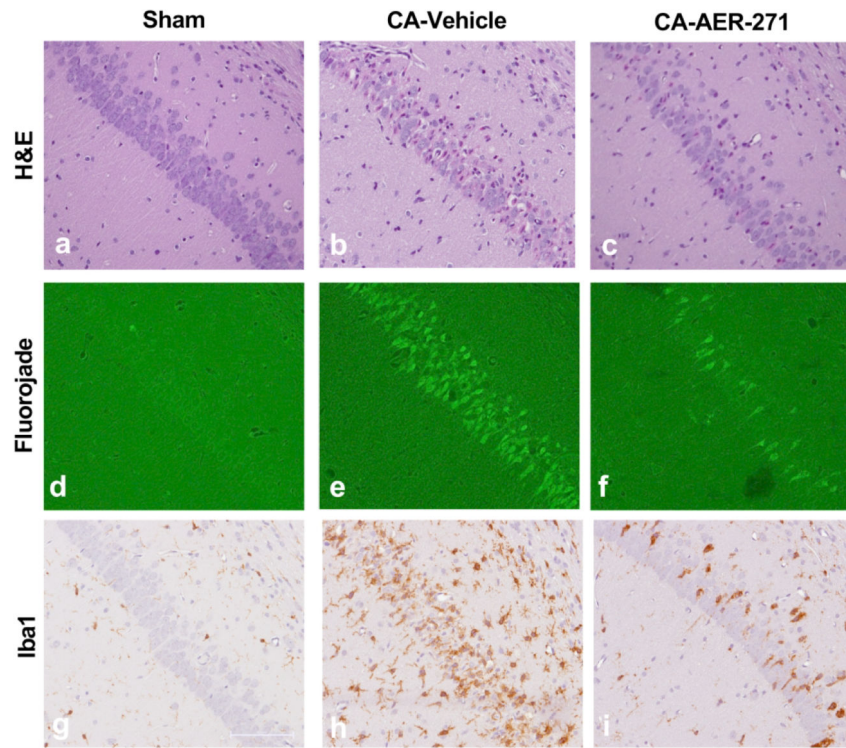


Figure 4. Representative sections and quantification of the histological assessment of the hippocampal CA1 region at 72 hours post-cardiac arrest. 20X magnification of hematoxylin & eosin (H&E) (a-c), fluorjode B (d-f), and Iba1 staining (g-i). Sham group is in the left column, vehicle group in the middle column, and AER-271 treatment group in the right column. Scale bar = 0.1mm shown in g.

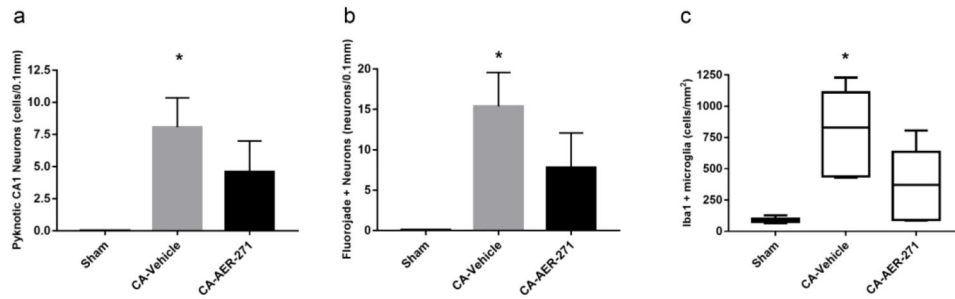


Figure 5.

Quantification of the histological assessment of the hippocampal CA1 region at 72 hours post-cardiac arrest. (a) H&E assessment of cell death. (b) Fluorojade assessment of neuronal injury. (c) Iba1 assessment of microglial response. Assessed by one-way ANOVA with Student Newman Keuls post-hoc test. Mean \pm standard error of the mean (H&E, FJB); Assessed by one-way ANOVA on Rank with Dunn's Method for pairwise multiple comparisons. Median [IQR] (Iba1); * p <0.05 vs Sham.

Table 1.

Study Design: treatment dosing and sample sizes by study outcome

OUTCOME	N	TREATMENT DOSING
Pharmacokinetic Studies		
IV vs IP Dosing	4/group	5mg/kg IP x2 (t=0 and 60 min post-ROSC)
IP + Infusion Pump	6/group	5mg/kg IP (t=0) + 0.08mg/h continuous
Edema		
3 h	6/group	5mg/kg IP x2 (t=0 and 60 min post-ROSC)
6 h	6/group	5mg/kg IP + 0.08mg/h continuous
24 h	6/group	5mg/kg IP + 0.08mg/h continuous
NDS and Histology	6/group	5mg/kg IP + 0.08mg/h continuous

Abbreviations: IV, intravenous; IP, intraperitoneal; mg, milligram; kg, kilogram; ROSC, return of spontaneous circulation